Mem. Natl Inst. Polar Res., Spec. Issue, 53, 157-176, 1998

COMPOSITIONAL ZONING AND ITS IMPLICATION IN A TOROIDAL CIRCULATION INSIDE THE YAKUSHIMA PLUTON, SW JAPAN

Ryo ANMA[1]*, Yoshinobu KAWANO[2] and Masaki YUHARA[3]

[1]*Hans Ramberg Tectonic Laboratory, Uppsala University, Villavagen 16, 75236 Uppsala, Sweden, and Department of Earth and Planetary Sciences, Tokyo Institute of Technology, Ookayama 2-chome, Meguro-ku, Tokyo 152-8551*
[2]*Faculty of Culture and Education, Saga University, Honjo 1, Saga 840-8502*
[3]*Graduate School of Science, Niigata University, 8050, Ikarashi 2-nocho, Niigata 950-2181*

Abstract: The epizonal Yakushima pluton at the north end of the Ryukyu arc displays an asymmetrical compositional zoning. The core and southeastern periphery of the pluton are per-aluminous cordierite granitoids, whereas the main constituent of the pluton is cordierite-free and rather primitive in Rb-Sr and Nd-Sm isotopes. This doughnut-like compositional zoning in the Yakushima pluton share the same symmetry as the patterns of magmatic flow fabrics defined by alignment of rigid orthoclase megacrysts, suggesting a single toroidal circulation cell about an axis inclined toward northwest.

Lithological contours inside this zoned pluton are locally truncated by the contours of intensities of solid-state deformation fabrics that developed during emplacement. Thus, the compositional zoning is likely to be inherited from an earlier stages of magmatic layering and relates the ascent processes.

This paper attributes the doughnut-like compositional zoning of the Yakushima pluton to the drag along the pluton's contact that circulated granite interior and formed the magmatic flow fabrics during its ascent. Such doughnut-like compositional zoning is expected in a magmatic pluton that rose through a ductile media as a diapir.

key words: compositional zoning, magmatic fabrics, diapir

1. Introduction

The origin of compositional zoning in granite plutons is an important issue among granite petrologists. Several mechanisms have been proposed to account for chemical heterogeneity in a magma body formed during the segregation, ascent and emplacement of granite melts.

Apart from the case of nested plutons, where lithological units have different ages with clear cross-cutting relationship, compositional zoning at the emplacement level may have been caused by assimilation of wall-rocks (contamination), flow differentiation (BHATTACHARJI, 1967), magma mingling after basal entrainment (ZORPI *et al.*, 1989; CRUDEN *et al.*,

*Present address: Institute of Geosciences, Tsukuba University, Tennodai, Tsukuba 305-8071.

1995) or differentiation due to cooling of the magma by sequential crystal settling (MARSH, 1988). In a static and homogeneous magma chamber, differentiation could take place through contamination and/or crystallization differentiation due to *in situ* cooling. A magma body dynamically circulated by viscous drag along its contact during intrusion, or because of post-emplacement thermal convection, may undergo flow differentiation.

"Normal", felsic-coreward, zoning is well explained by differentiation by crystal settling and/or marginal accretion of crystalline phases during cooling. In contrast, "reverse", mafic-coreward, zoning has been attributed to the process of flow differentiation or magma mingling. FRIDRICH and MAHOOD (1984) explained reverse zoning in the central intrusion of the Grizzly Peak cauldron in terms of the rearrangement of a vertical gradient in magma composition into a mafic-coreward zonation during the laccolithic emplacement of the central intrusion. Their idea was later succeeded and developed by ZORPI *et al.* (1989) and CRUDEN *et al.* (1995).

In this paper, we use structural and petrological constraints to discuss the mechanism responsible for a doughnut-like compositional zoning in the island arc Yakushima pluton.

2. Tectonic Settings

The Yakushima granite is one of the products of a Miocene plutonic activity that took place in the brief time span between 15 and 12 Ma (SHIBATA, 1978) in the Outer Zone of Southwest Japan. The Yakushima pluton, ≈ 400 km^2 in exposure, is located only 170 km behind the axis of the Ryukyu trench, between the trench and a chain of active volcanoes (Fig. 1a, b).

At the map scale, the Yakushima pluton cuts across structures in its wall rocks of Cretaceous-Oligocene deep-clastic sediments of the Shimanto group that strike NNE-SSW (Fig. 1b). There seems to be no significant control on the intrusion by these pre-emplacement structures. Instead, the pluton arched pre-emplacement wall-rock structures that developed during accretion (ANMA, 1997). Outside its smoothly elliptical planform, the pluton has a narrow (≈ 4 km) thermal metamorphic aureole. Granitoid apophyses up to 2 m-wide, extend several hundred meters from the pluton. These observations suggest that hot granite with low viscosity was able to move considerable distance in such apophyses to intrude cool and brittle sedimentary rocks at shallow depth.

3. Primary Flow Fabrics

The magmatic fabrics within the pluton (Fig. 2) were used to infer the mechanism of emplacement of the Yakushima pluton (ANMA, 1997) into a thin brittle upper crust (≈ 15 km thick; IWASAKI *et al.*, 1990) of the island arc overriding a viscous lower crust and weak mantle (SHIMAMOTO, 1993).

Orthoclase megacrysts in the Yakushima pluton have a rectangular platy shape with a mean aspect ratio of about 3 : 3 : 1 and provide excellent flow markers. The local flow fabric defined by the alignment of the megacrysts was used to generate an S-pole configuration on a Schmidt net for each 1 km^2 of the pluton. S-pole concentrations were used to map the orientation, and to define the shape (K-value) and intensity of fabric alignment resulting from magmatic flow in each domain (Fig. 2; see ANMA, 1997 for

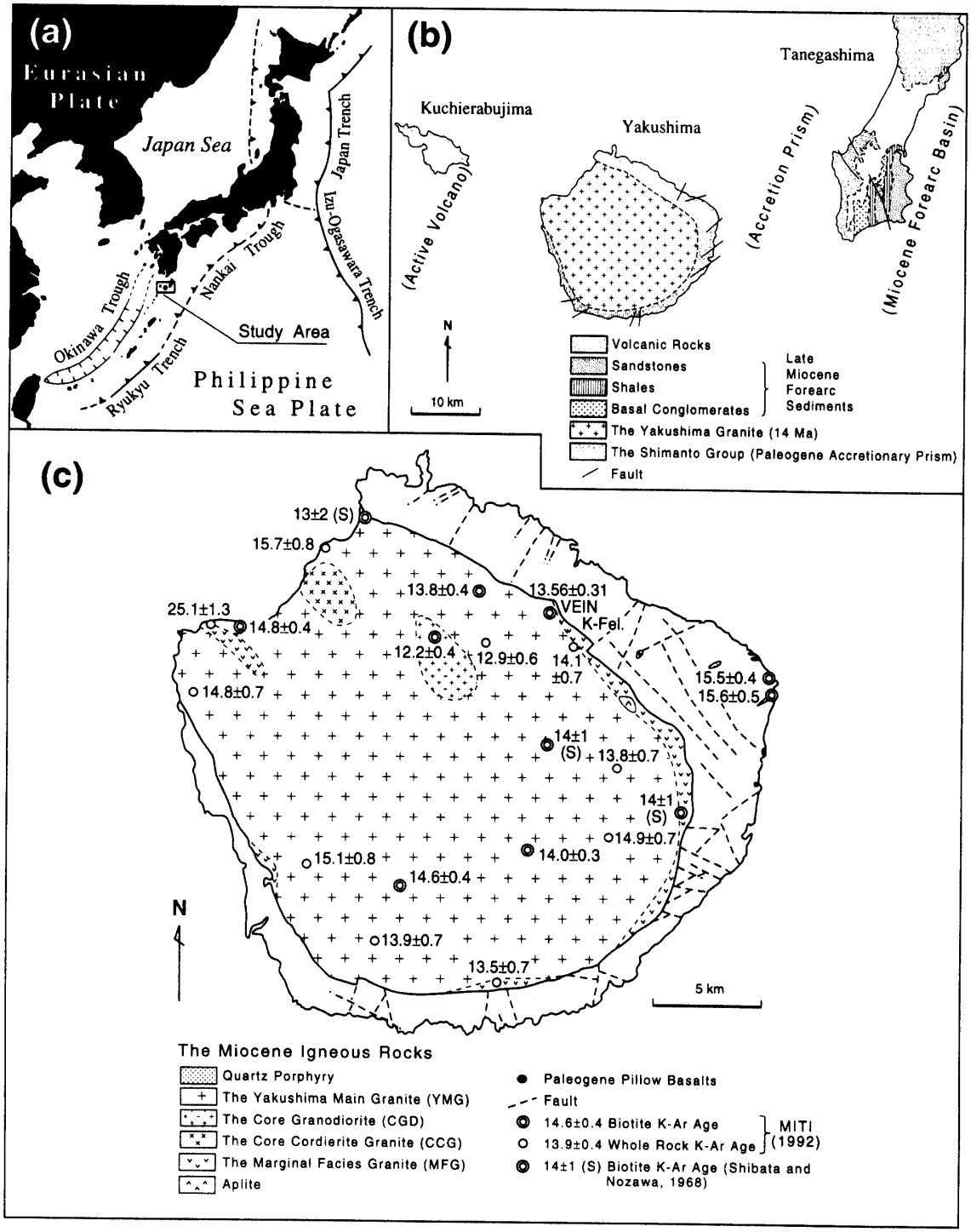

Fig. 1. *(a) Map showing regional plate configurations and location of Yakushima. The Yakushima pluton is located at the northern tip of the Ryukyu island arc. (b) Tectonic setting and geology of the Yakushima granite. Patterns used for the Shimanto group and Miocene shales are parallel to strikes of bedding planes. On this view, the structures in the Shimanto group are truncated by the granite contact with its smoothly circular planform. A chain of active volcanoes (Tokara volcanic arc) extends northeast and southwest from Kuchi-erabujima. The Miocene forearc basin extends north-northeast parallel to the Ryukyu trench. (c) Lithology and ages of the Yakushima pluton (see text for details).*

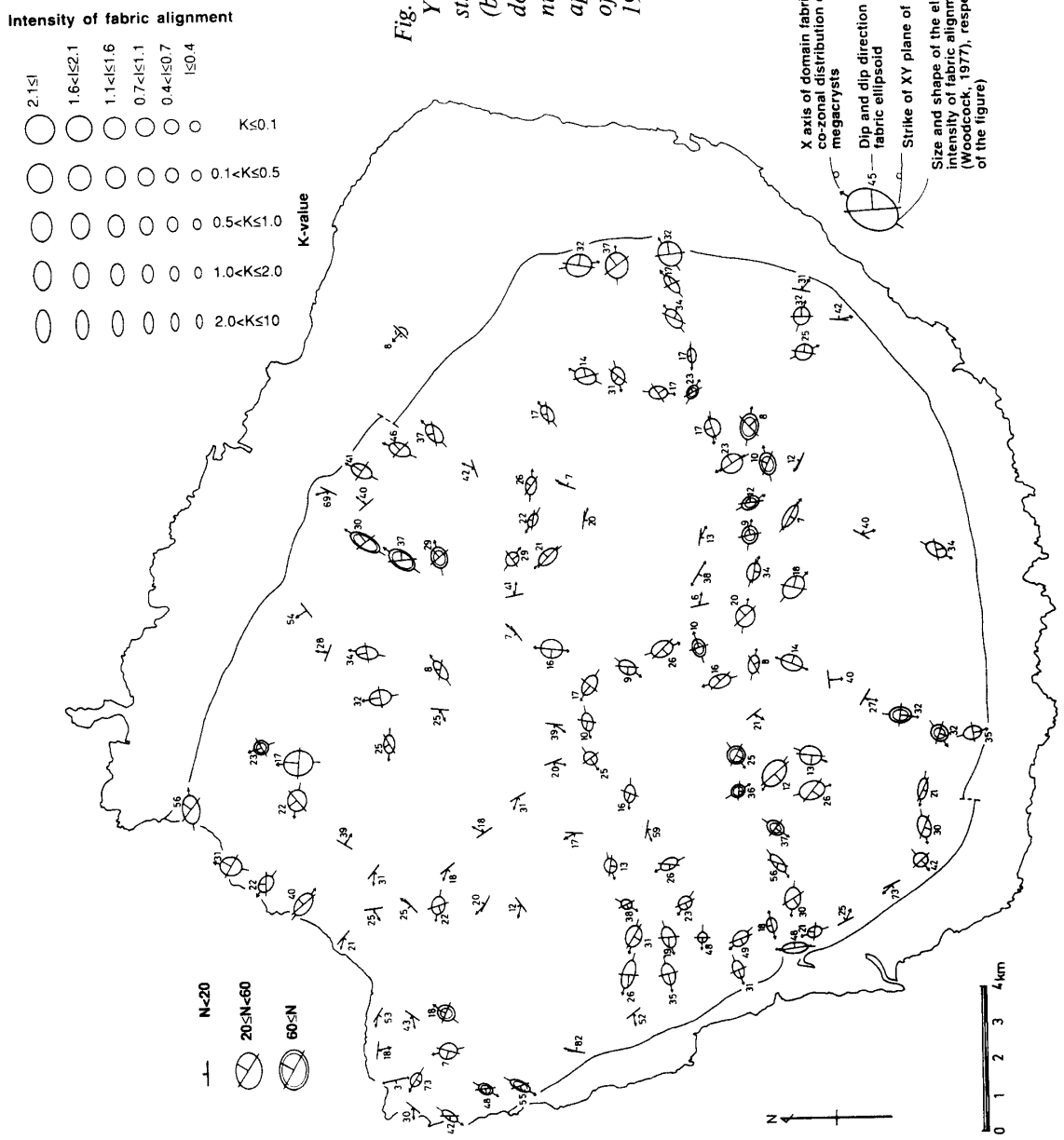

Fig. 2. Domain fabric ellipsoids in the Yakushima granite: dips (in degrees) and strikes of XY planes, directions of X axes (bottom-right), shape and intensity of domain fabric ellipsoids (top-right) and the number of measurements (top-left) that approximate the reliability of estimation of the domain fabric ellipsoids (see ANMA, 1997, for detail) are shown.

details).

The results of 129 analyses of the primary flow fabric (Fig. 2) showed that: (1) the overall orientations and shapes of the domain fabric ellipsoids suggest that the exposed Yakushima pluton is the crest of a domal structure; (2) domain fabric ellipsoids were strongly oblate only in the eastern marginal zone of the pluton; (3) the XY plane of the domain ellipsoids ($X \geq Y \geq Z$) dip outward and the X axes plunge outward, in particular, at the northeastern and southwestern margins where X axes display a constant northeast-southwest trend; (4) the magmatic flow fabric is generally symmetric about a centreline trending northwest-southeast; and (5) XY planes of domain ellipsoids in the centre of the pluton dip inward toward the centreline.

The patterns of flow structure inside the Yakushima pluton resemble those of internal deformation theoretically expected in an active buoyant diapir (see Section 6). ANMA (1997) concluded that the Yakushima pluton emplaced diapirically. However, the mechanism for the magma transportation from the depth of magma segregation remained unsolved, since the floating and rotating megacrysts in a granite melt have a short strain memory and thus, these primary flow fabrics must have formed during the emplacement of the pluton. In the following sections, we describe compositional zoning of the Yakushima pluton, that may record the processes during the segregation and ascent of the granite melts.

4. Petrography, Textures and Cooling Ages

The rocks of the Yakushima pluton are classified as S-type ilmenite-series calk-alkaline granites (CHAPPELL and WHITE, 1974; ISHIHARA, 1977; NAKATA and TAKAHASHI, 1979; TAKAHASHI *et al.*, 1980; KAWANO, 1991). There are four components in the pluton (Fig. 1c): the Yakushima main granite (YMG), the core granodiorite (CGD), the core cordierite granite (CCG; identified during this study) in the north end of the island, and the marginal facies granite (MFG; the Aiko-dake granite of SATO *et al.* (1982)). The core granodiorite and core cordierite granite were considered together as the Yoshida granodiorite by SATO *et al.* (1982). However, we argue here that they are separate bodies that have different textural and chemical characteristics. To simplify our description, we hereafter will use abbreviations YMG, CGD, MFG and CCG for each granite and the term "Yakushima pluton" for the whole body. The petrographies, textures and cooling ages of each rock type are described below. Localities of thin section stations are indicated in Fig. 3.

3.1. Yakushima main granite (YMG)

The Yakushima main granite (YMG) occupies 90% of the total planform area of the Yakushima pluton (Fig. 1c). This granite is a coarse-grained orthoclase-porphyritic biotite granite (SATO *et al.*, 1982) and appears to be homogeneous. Constituent minerals are plagioclase of andesine to albite composition, quartz, potassium feldspar (both in groundmass and as megacrysts) and biotite. They have a general grain size of around 5 mm in diameter and exhibit hypidiomorphic granular textures. Muscovite, chlorite, ilmenite, zircon and apatite occur as accessory minerals. Tourmaline is found in three YMG thin sections out of 75 (Fig. 3, indicated by T).

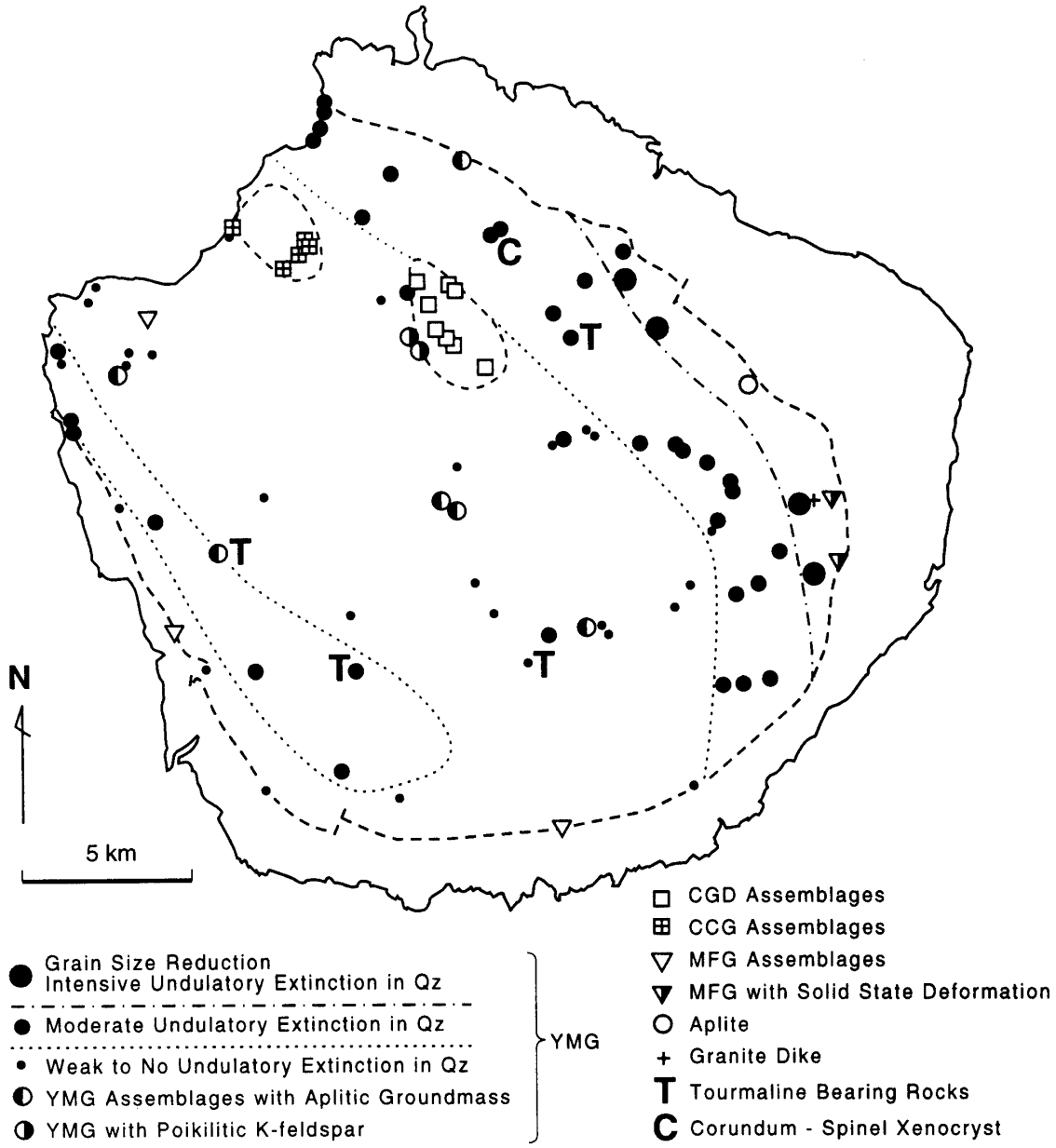

Fig. 3. Thin section stations, assemblages and deformation fabrics in the Yakushima pluton. Intensive solid-state deformation took place along the northeastern periphery of the pluton. Contours of the intensity of this emplacement-related deformation fabrics cut across lithological boundaries in Fig. 1. Six out of 75 thin sections of the YMG show aplitic groundmass texture around phenocrysts of the YMG assemblages.

The YMG contains around 7 modal percent of orthoclase megacrysts (KAWACHI and SATO, 1978; SATO and NAGAHAMA, 1979). The megacrysts are euhedral perthitic feldspar with a diameter up to 14 cm. These orthoclase megacrysts were suggested to date from the earliest phase of crystallization (KAWACHI and SATO, 1978) under high pressure ($\approx$ 10 kb) and high water content ($\approx$ 10%).

Subhedral plagioclase shows general normal zoning texture with minor oscillation in a compositional range usually varying from An_{35} to $An_{\approx 0}$. Quartz crystals are subhedral to anhedral grains that usually exhibit weak to moderate undulatory extinction. Intensive undulatory extinction was observed along the northeastern periphery of the pluton (Fig. 3) where local grain-size reduction was observed and the orthoclase megacrysts exhibited strong parallelism in the outcrop (Fig. 2).

K-Ar ages of the rocks of the YMG range from 13.8 to 14.8 ± 0.4 Ma (n=4) using biotite, and from 13.5 to 15.7 ± 0.8 Ma (n=8) using the whole rock method (Fig. 1c; MITI, 1992).

3.2. Core granodiorite (CGD)

The core granodiorite (CGD) is surrounded by the YMG in the north-central part of the pluton (Fig. 1c). The CGD is a medium-grained orthoclase-porphyritic cordierite muscovite biotite granodiorite (SATO *et al.*, 1982). Constituents are plagioclase of andesine to albite composition (phenocrysts and groundmass), quartz, potassium feldspar (mostly as megacrysts that occupy 1 to 2 modal percent of the CGD and as groundmass crystals), biotite, muscovite and cordierite. Plagioclase crystals in the CGD are euhedral to subhedral and have $\approx An_{30}$ cores surrounded by $\approx An_{50}$ rims in which the An content decreases to An_2 toward the crystal boundary.

The CGD is dated at 12.2 ± 0.4 Ma (K-Ar biotite age; MITI, 1992). This is the youngest cooling age among the igneous rocks on Yakushima (Fig. 1c).

3.3. Core cordierite granite (CCG)

The CCG is similar to the CGD in the outcrops. However, megacrysts in the CCG consist of both orthoclase and glomeroporphyritic plagioclase feldspars.

Groundmass quartz crystals, less than 1 mm in diameter, in the CCG show two modes of occurrences: 1) subhedral to anhedral magmatic crystals, and 2) scattered subhedral quartz grains which may be inherited from protolith. Groundmass potassium feldspar crystals, commonly seen, are poikilitic with scattered quartz grains. Both fresh and sericitized euhedral to subhedral plagioclase crystals were observed in the groundmass. They have a distinctive rim ($\approx An_{52}$ that decreases to An_{15} toward the grain boundary) around a homogeneous core of $\approx An_{33}$. The An_{30} core of plagioclase often contains laths of sillimanite that do not parallel either the zonal texture or twinning plane. Scattered quartz grains are distributed along the boundary between the high-An rim and low-An core. Cordierite is common. A cluster of garnet-cordierite-biotite-(muscovite) grains was observed in the CCG.

3.4. Transition zone between the CGD, CCG and YMG

The boundary between the CGD and YMG and between the CCG and YMG can be constrained with an accuracy of ± 100 m. However, we found no outcrop with cross-cutting relationships. Instead, there seems to be a zone of indeterminate width where the YMG is contaminated by the CGD and/or CCG. Textures and field appearances of the rocks in this zone are similar to those of the YMG. However, the rocks in this zone contain clots of subhedral muscovite grains. Calcite occurs as intercrystalline fillings. In a couple of thin sections from just west of the CGD (Fig. 3), groundmass potassium

feldspar crystals are poikilitic with scattered quartz grains, as in the CCG. An assemblage of corundum-hercynite-biotite-muscovite-plagioclase was found as a ghost of a xenocryst in this zone (marked by C in Fig. 3).

3.5. *Marginal facies granite (MFG)*

The marginal facies granites (MFG) are in contact with the sedimentary rocks of the Shimanto group along the eastern and southwestern periphery of the pluton (Fig. 1c). The MFG is an orthoclase-porphyritic cordierite-bearing muscovite biotite granite. The only distinctive difference between the YMG and MFG is the occurrence of cordierite.

Table 1. Major and trace element compositions, Sr and Nd isotope ratios for Yakushima.

	YMG (av. $n=26$)	CGD (av. $n=3$)	CCG (av. $n=2$)	MFG (av. $n=2$)	G. Dike
SiO_2	70.92	71.52	71.26	72.31	70.85
TiO_2	0.55	0.40	0.42	0.54	0.26
Al_2O_3	14.34	14.98	14.50	13.86	15.41
Fe_2O_3	0.47	0.40	0.33	0.57	0.03
FeO	2.61	1.77	2.34	2.45	1.38
MnO	0.07	0.05	0.07	0.07	0.05
MgO	0.86	0.75	0.95	0.76	0.61
CaO	2.17	2.05	1.95	1.89	1.67
Na_2O	3.22	3.37	2.99	2.98	4.07
K_2O	3.85	3.23	3.11	3.71	4.29
P_2O_5	0.14	0.10	0.12	0.15	0.08
L.O.I.	0.61	0.84	1.26	0.52	0.44
Total	99.75	99.45	99.27	99.79	99.14
Ba	257	319	410	211	135
Cr	37	52	71	51	33
Cu	4	0	8	0	0
Nb	9.7	3.3	7.0	6.3	4.7
Ni	6	4	8	6	3
Rb	183	164	126	192	211
Sr	154	191	223	133	111
Y	40	21	22	41	46
Zn	51	50	45	48	42
Zr	170	137	131	169	95
Nd	*26.3	18.6	22.9	28.4	21.7
Sm	*5.5	3.6	4.3	5.4	5.2
$^{143}Nd/^{144}Nd$	*0.512427	0.512368	0.512287	0.512384	0.512417
$^{87}Sr/^{86}Sr$	*0.70826	0.70811	0.70993	0.70924	0.70902

Note: YMG=the Yakushima Main Granite; CGD=the Core Granodiorite; CCG=the Core Cordierite Granite; MFG=the Marginal Facies Granite; G. Dike=Granite Dike in YMG. Units: major elements in % and minor elements in ppm. *$n=13$.

Fabrics in the MFG share similar characteristics with the neighbouring YMG. Thus, along the eastern margin of the Yakushima pluton, both the YMG and neighbouring MFG show strong undulatory extinction in quartz grains and localized grain-size reduction in rocks deformed in similar manners (Fig. 3). Plagioclase crystals show general normal zoning with minor oscillations in a composition range decreasing from An_{49} in the cores to An_{11} in the rims.

A thin section from the southernmost part of the MFG shows a similar texture to the rocks of the CCG. As in the CCG, scattered quartz grains less than 0.2 mm in diameter are observed within feldspar grains. This thin section also contains garnet and cordierite crystals accompanied by sericite.

3.6. Late granite dikes

Along the eastern periphery of the pluton, late granite dikes intruded the host YMG parallel to the plutonic contact (at locality indicated in Fig. 3). They are free of orthoclase megacrysts. The compositions of plagioclase crystals from a dike decrease from An_{27} in the cores to An_1 in the rims.

4. Petrology of the Yakushima Pluton

4.1. Major and trace element compositions

Major and trace element compositions were measured using an X-ray fluorescence spectrometer at the Niigata University. FeO and loss on ignition were measured by conventional wet chemical methods. Four samples were selected for the neutron activation analysis of rare earth elements (REEs). Representative analytical results are listed in Table 1 (for major and trace elements) and Table 2 (for REEs).

The SiO_2 contents of the granitic rocks of the Yakushima pluton range between 66% and 76%. These granites contain less MnO and Na_2O, and more TiO_2 and $FeO+Fe_2O_3$ than is normal for Cretaceous-Paleogene Japanese granites (ARAMAKI *et al.*, 1972). With the exception of Al_2O_3, Harker plots for major and trace elements (Fig. 4a and b respectively) show wide scatter and very weak variation trends for each lithology. Nevertheless, the Harker plots show the fundamental characteristics of each lithological unit and allow the

Table 2. Rare earth elements for Yakushima.

Sample	YMG 0302	YMG 0902	CGD 0505	G. Dike 1401
La	32.0	31.9	31.4	19.8
Ce	78.3	91.5	78.8	43.6
Sm	5.5	5.3	4.5	5.2
Eu	1.0	1.0	1.1	0.7
Yb	3.2	3.1	n.d.	3.6
Lu	0.53	0.44	0.32	0.51

Note: YMG=the Yakushima Mian Granite; CGD=the Core Granodiorite; G. Dike=Grainte Dike. Unit: in ppm.

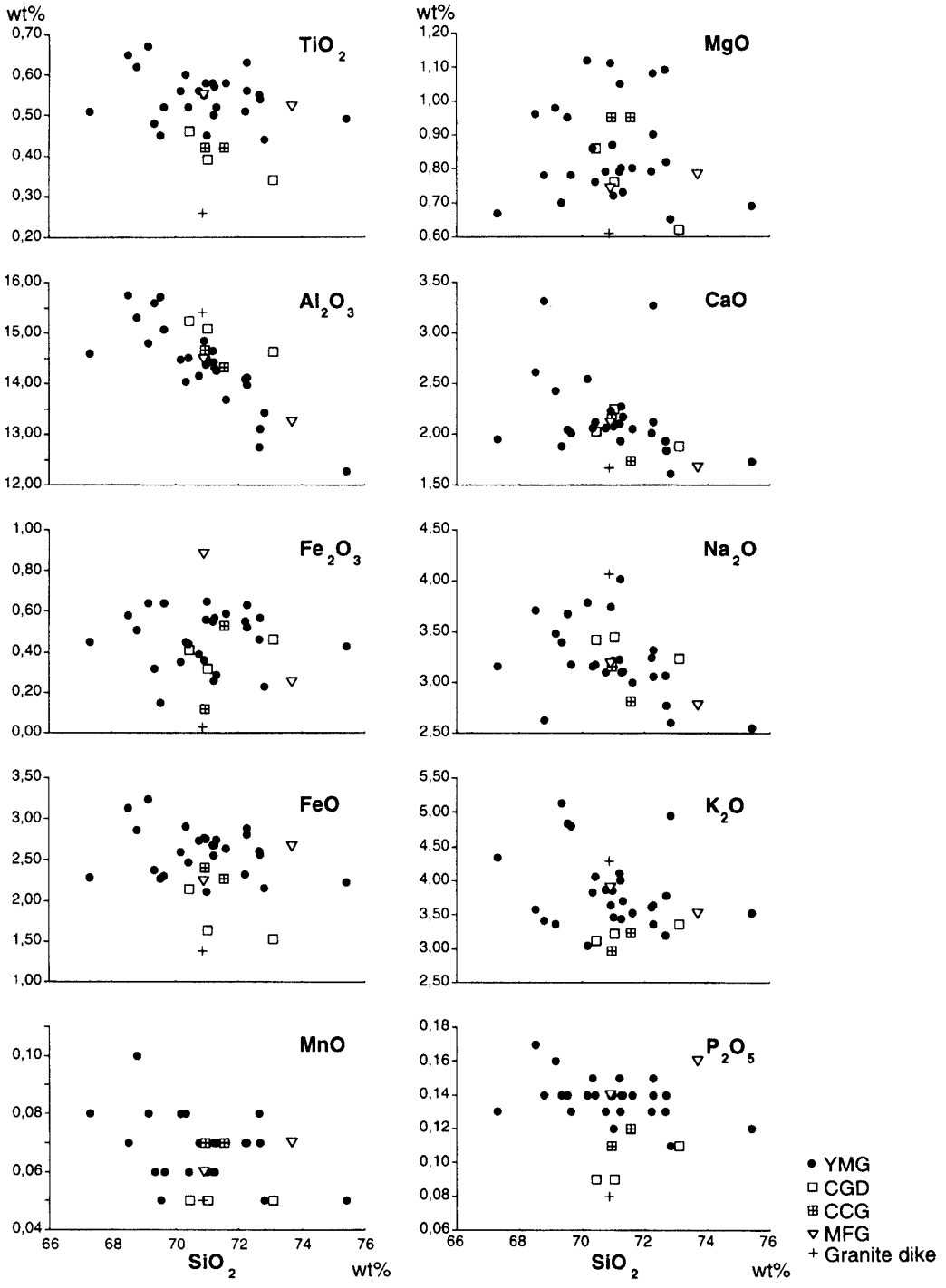

Fig. 4a

Fig. 4. (a) Harker plots for major elements have very weak variation trend except for Al. The CGD contains more than 15% Al_2O_3 at the 70% SiO_2 level. The Al contents decrease in the order: CGD, CCG, MFG and YMG. Fe, Mg and Mn are concentrated in the YMG, MFG and CCG (see text for details). (b) Harker plots for trace elements. High strength field elements like Nb, Zr and P concentrate in the YMG, as Rb and Y. · The CGD and CCG are rich in Ba, Cr and Sr (see text for details).

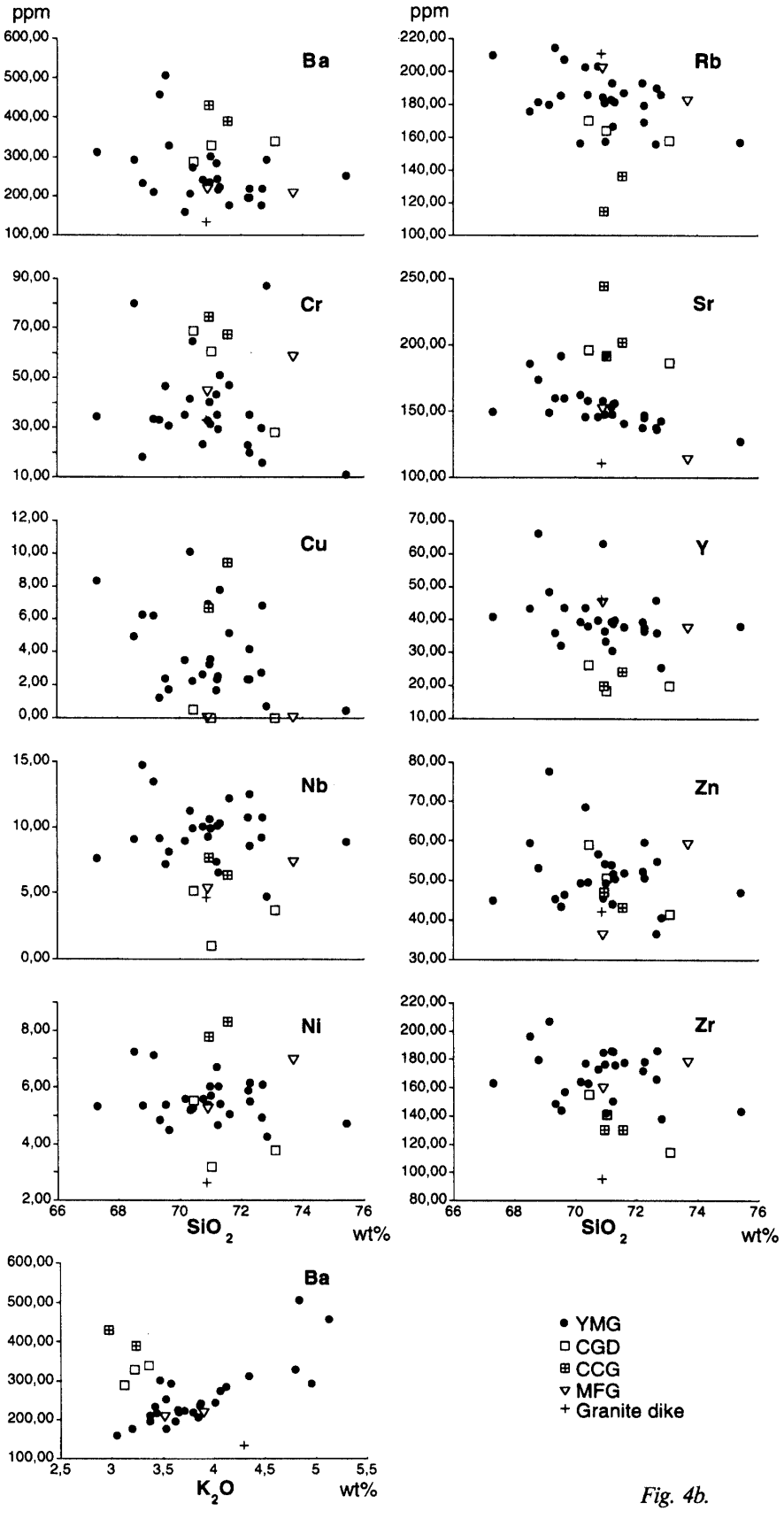
ppm
Ba
600,00
500,00
400,00
300,00
200,00
100,00
ppm
Rb
220,00
200,00
180,00
160,00
140,00
120,00
100,00
Cr
90,00
70,00
50,00
30,00
10,00
Sr
250,00
200,00
150,00
100,00
Cu
12,00
10,00
8,00
6,00
4,00
2,00
0,00
Y
70,00
60,00
50,00
40,00
30,00
20,00
10,00
Nb
15,00
10,00
5,00
0,00
Zn
80,00
70,00
60,00
50,00
40,00
30,00
Ni
8,00
6,00
4,00
2,00
Zr
220,00
200,00
180,00
160,00
140,00
120,00
100,00
80,00
66 68 70 72 74 76
SiO2 wt%
66 68 70 72 74 76
SiO2 wt%
Ba
600,00
500,00
400,00
300,00
200,00
100,00
2,5 3 3,5 4 4,5 5 5,5
K2O wt%
• YMG
□ CGD
⊞ CCG
▽ MFG
+ Granite dike

Fig. 4b.

following observation.

Al_2O_3 contents in the rocks of the Yakushima pluton decrease rapidly with increasing SiO_2. They decrease in the order: CGD, CCG, MFG and YMG, and reflect the peraluminous nature of the first three granites. The CGD contains more than 15% Al_2O_3 at the 70% SiO_2 level. Ferro-magnesian elements are concentrated in the YMG, MFG and CCG, and decrease toward the late granite dikes. Total alkali+CaO is higher in the YMG and granite dike, and lower in the MFG, CGD and CCG. The late granite dike is poorer in TiO_2, $FeO+Fe_2O_3$, MgO, CaO and P_2O_5, and richer in Na_2O and K_2O than the earlier granitoids.

Figure 5 shows a normative An-Ab-Or diagram for the rocks of the Yakushima pluton. The YMG samples plot on the boundary between the granodiorite and granite fields, whereas CGD samples are abundant in the Ab-An components and are shifted toward the tonalite-trondhjemite field. A rock from the orthoclase-free granite dike plots in the granite field.

Patterns of enrichment in trace elements show interesting characteristics (Fig. 4b). High-field strength (HFS) elements like Nb and Zr (also P and Sn; See SATO *et al.*, 1982) concentrate in the YMG, whereas the MFG, CCG, CGD and the late granite dike are depleted in HFS elements in this order. In contrast, large ion lithophile (LIL) elements such as Ba and Rb (also potassium) have complicated distributions. Ba is concentrated in the CGD and CCG, whereas Rb and K are concentrated in the YMG, MFG and the granite dike. A plot of Ba contents against potassium (Fig. 4b) shows clearly that the CGD and CCG are enriched in Ba. Sr is also concentrated in the CGD and CCG. A plot of Sr contents against Rb contents (Fig. 6) shows enrichment of Rb in the YMG, MFG and the granite dike, whereas the CCG is most depleted. The CGD and CCG share similar characteristics except for Cu and Ni.

Comparison between REE concentrations in each granitoid (Table 2) shows that the YMG and CGD are richer in light REE (like La and Ce with large ion size) than the granite dike and that the CGD is depleted in heavy REE (like Yb and Lu).

4.2. Rb-Sr and Nd-Sm isotope systems

We extracted and separated Sm and Nd for isotopic analyses following the procedure

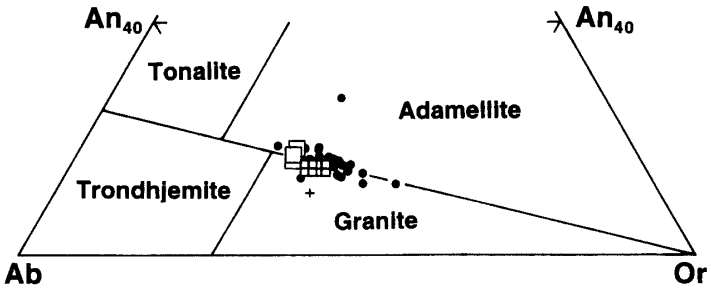

Fig. 5. A normative An-Ab-Or diagram for Yakushima. Solid lines separating various rock types are after O'CORNER (1965). The YMGs plot on the dividing line between fields for adamellite and granite, whereas a specimen from the granitic dike plots in the granite field. The rocks of the CGD are shifted toward the tonalite-trondhjemite field compare to the YMGs. Symbols are the same as in Fig. 3.

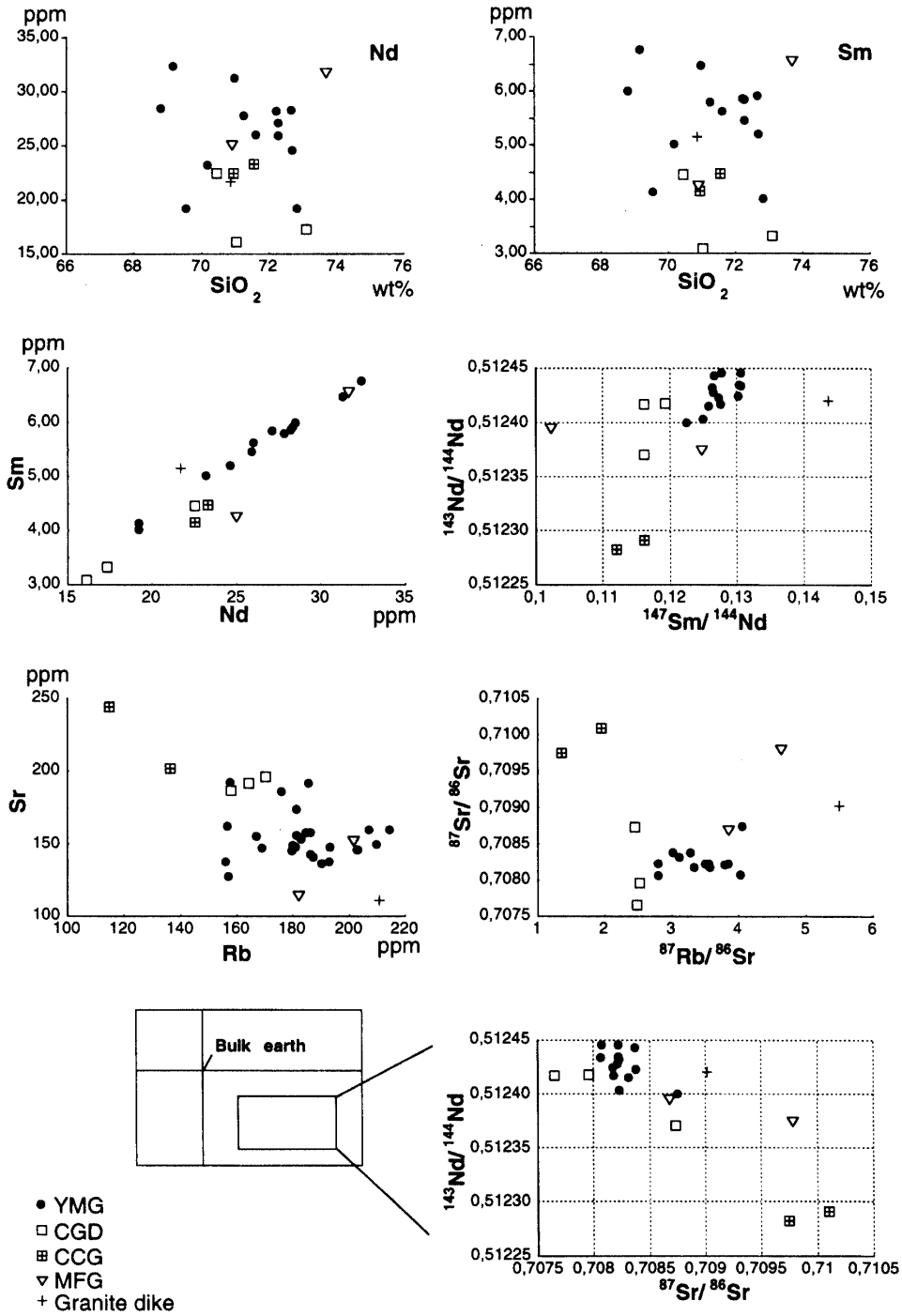

Fig. 6. Plots for Sr and Nd isotopes show a wide scatter typical of S-type granites. The CCG has the highest Sr isotope ratio, suggesting that it is contaminated by protoliths. The CCG is also distinctive in Nd isotopes (see text for details).

given by KAGAMI *et al.* (1987, 1989). Isotopic analyses were carried out using a MAT261-type mass spectrometer at the Institute for Study of the Earth's Interior, Okayama University.

All the rocks of the Yakushima pluton have significantly lower Nd and higher Sr

isotope ratios than that of the bulk earth. The wide scatter in Rb-Sr isotopes is a characteristic of S-type granitoid plutons and prevents us from drawing any isochron (Fig. 6). However, the CCG obviously has the highest strontium isotope ratio (around 0.7095) among the granitoids in the Yakushima pluton, whereas that of the YMG is around 0.7075 (Fig. 6). The CCG has the lowest $^{87}Rb/^{86}Sr$ value. The CGD is also depleted in Rb but has a lower $^{87}Sr/^{86}Sr$ value than the CCG. The MFG is enriched in Rb and has higher $^{87}Sr/^{86}Sr$ values than the YMG.

A plot of Sm-Nd isotope ratios shows similar characteristics (Fig. 6). The CCG and CGD are depleted in Sm. The Sm/Nd ratio is the highest in the granite dike and decreases in the YMG with the lowest values in the MFG, CGD and CCG. The CCG has the lowest $^{143}Nd/^{144}Nd$ value, whereas those of CGDs are higher and similar to those of the YMGs. The MFG has a similar $^{143}Nd/^{144}Nd$ value to the CGD and is depleted in Sm. The late granite dike is enriched in both Rb and Sm and has relatively high $^{87}Sr/^{86}Sr$ and $^{143}Nd/^{144}Nd$ values.

A conventional plot of $^{143}Nd/^{144}Nd$ against $^{87}Sr/^{86}Sr$ shows that the CCG has isotope characteristics closest to the sedimentary rocks of the Shimanto group (TERAKADO *et al.*, 1988).

5. Interpretation

Although the rocks of the core granodiorite (CGD) and the garnet-bearing cordierite granite (CCG) in the northern end of the Yakushima pluton are separated from the cordierite-bearing marginal facies granites (MFG) in the periphery by the intervening the volatile-rich Yakushima main granite (YMG), the former three are all cordierite-bearing per-aluminous granitoids. Plagioclase grains in the CGD, CCG and MFG have a higher An content than plagioclase in the YMG, although their host rocks are poorer in bulk CaO than the YMG. This implies that temperature of crystallization was higher in the core and peripheries of the pluton. Therefore, the Yakushima pluton seems to have a doughnut-like zoning pattern. The symmetry of the compositional zoning, however, is not radial but bilateral about an NW-SE axis: *i.e.* the CGD and CCG are distributed in the northern part of the pluton, whereas the MFG is distributed along the southeastern periphery of the pluton.

The Sm-Nd and Rb-Sr isotope studies indicate that the YMG is the most primitive granitoid in the Yakushima pluton, although they all have much higher Sr and lower Nd isotope ratios than the bulk earth. The MFG and YMG share similar texture and compositional variations, but the MFG deviate from the YMG in isotopes. A thin section in the MFG exhibits similar textures to these in the CCG that has the closest Sm-Nd and Rb-Sr isotopes to the sedimentary rocks of the surrounding Shimanto group. The CGD and CCG share similar compositional characteristics, but the CGD appears to be more primitive in isotope ratios than the CCG.

The rocks of the S-type Yakushima pluton are likely derived from the melting of crustal rocks from its mineral assemblages, chemical compositions and isotopic characteristics. Textural studies under the optical microscope revealed the presence of small quartz grains scattered through the poikilitic K-feldspar and plagioclase in the CCG and supports the idea that the CCG is contaminated by restitic material from its crustal protolith±

sediments. Exposures of the CCG appear to be continuous from ≈200 m to more than 600 m above sea level. In contrast, rocks with the highest metamorphic grade are exposed around the pluton up to 300 m above sea level, and are merely andalusite-bearing cordierite biotite hornfels (ANMA, 1997). Therefore, it is almost impossible to attribute the CCG to the melting of a huge xenolith which sank from the roof of the Yakushima pluton. Plagioclase mineralogy also disagree with this central zoning being due to the *in-situ* contamination at the emplacement level. The process that generated the melt of the CCG must have been deep.

6. Discussion: Mechanism Responsible for the Compositional Zoning of the Yakushima Pluton

An obvious question concerning the mechanism of intrusion responsible for the compositional zoning remains; whether the Yakushima pluton is a set of the nested plutons, a single diapir with a doughnut-like compositional zoning due to internal circulation, or a pluton resulting from a continuous magma supply through a conduit or fracture system (ballooning or laccolith). The youngest cooling age of the CGD (Fig. 1c; MITI, 1992) raises the possibility that the CGD was added from below after the emplacement of the YMG. The fabrics defined by the alignment of orthoclase megacrysts (Section 3) and solid-state deformation fabrics within the pluton (Section 4) resolve this problem.

Variations in orientation and shape of neighbouring domain ellipsoids (Fig. 2) across the contacts between internal lithological units (Fig. 1c) appear sufficiently smooth to assume that there was no significant viscosity contrast during magmatic flow of the various granitoids making up the Yakushima pluton. The outward-trending prolate domain ellipsoids typical of the northeastern and southwestern parts of the periphery of the pluton (Fig. 2) are not the pattern expected in either simple ballooning (point dilation) of magma plutons (RAMSAY, 1989) or laccolithic inflation (FINK, 1983; FINK and POLLARD, 1983). These observations also eliminate the possibility of the Yakushima pluton being a nested pluton, where strong oblate-type ellipsoids are expected near the contacts of successive units with different viscosities. Furthermore, the textures in the YMG around the CGD and CCG are mostly magmatic and exhibit few traces of solid state flow (Fig. 3).

The lithological boundaries of this zoned pluton (Fig. 1c) are locally truncated by the contours of intensities of the emplacement-related solid-state deformation fabrics (Fig. 3). This independently suggests that the compositional zoning of the pluton was not due only to a process at the final-emplacement level, but involved an earlier and deeper process.

The flow structure inside the Yakushima pluton (Fig. 2) resembles the pattern of internal deformation theoretically expected in an active buoyant diapir (TALBOT and JACKSON, 1987; SCHMELING *et al.*, 1988; CRUDEN, 1990; WEINBERG, 1992: ANMA, 1997). A simplified dynamic model of viscous spheres rising through viscous surroundings (Fig. 7a) shows uniaxial constriction occurring up the centre-line of a rising sphere, changing to axial flattening at its crestal stagnant point, followed by non-coaxial flattening accompanied by lateral extension around the equator of its outer contact.

Figure 7b illustrates a possible interpretation of the 2D flow pattern within the Yakushima granite that fits a section of the simple 3D dynamic model in Fig. 7a. Comparison between Fig. 7a and 7b shows the following similarities: (1) the circular axis

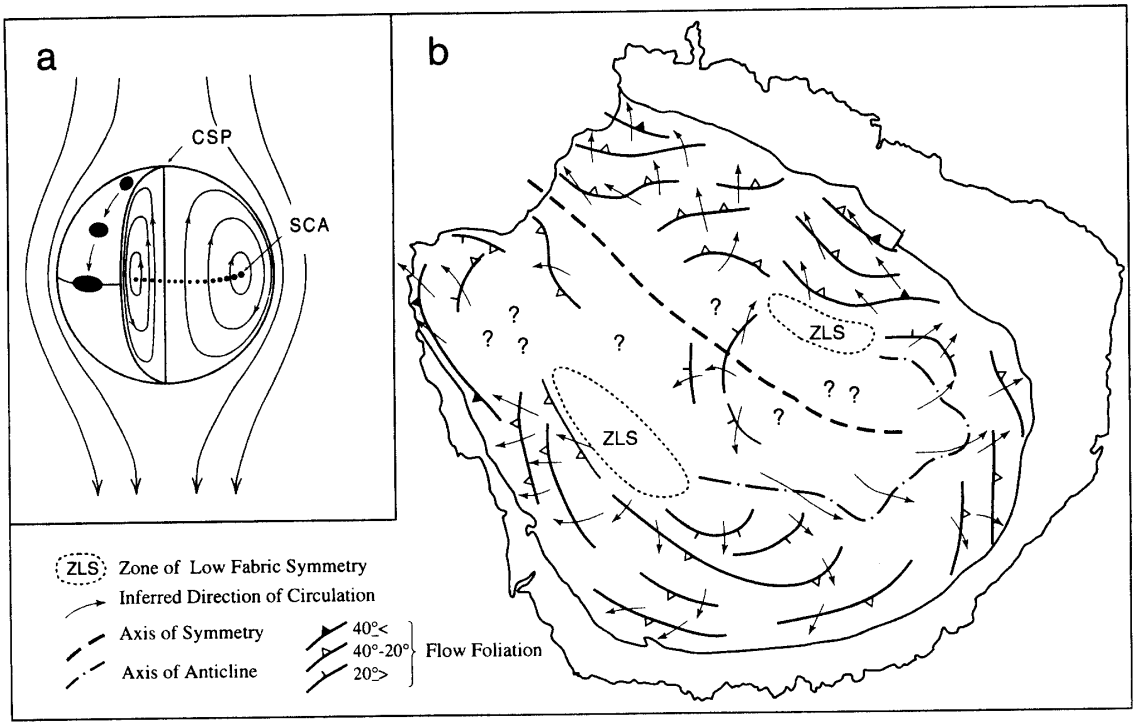

Fig. 7. (a) Flows inside a rising Stokes sphere are expected to involve strong flattening at the crestal stagnant point (CSP) and rotational strain around the stagnant circular axis (SCA). Circular passive markers carried from the crest of the sphere to its equator deform to ellipses parallel to the equator. (b) A possible interpretation of the flow structure inside the Yakushima pluton. Zones of low strain (ZLS) coincide with the SCA. Inward dips at the centre of the pluton imply overturn in toroidal circulation. A general mirror symmetry about the southeast trending midline of the elliptical granite is attributed to oblique rise of the pluton up to the southeastward. Thin arrows indicate the local direction of internal circulation (ANMA, 1997; copyright: Kluwer Academic Publishers).

of stagnant flow in the torus of circulation is recognizable as two zones of low fabric symmetry; (2) strong oblate ellipsoids in the eastern periphery of the pluton (Fig. 2) correspond to the crestal stagnant point; (3) relatively strong plane fabric symmetry with axes constant along the NW-SE mid-line of the pluton are interpreted as being due to the central upwelling nearby; and (4) prolate ellipsoids around the periphery can be attributed to non-coaxial deformation normal to the longest axis of the domain ellipsoid.

The symmetry of the flow fabric on a map (Fig. 7b), interpreted as a 2D section of the 3D theoretical model (Fig. 7a), is not radial as expected of a vertically emplaced diapir. Instead, it is bilateral along the NW-SE axis of the slightly elliptical planform of the Yakushima pluton. This geometry of emplacement-related structure, indicating that the granite interior was circulated about an axis inclined toward NW, shares the same symmetry as the pattern of the compositional zoning that relates a deeper process.

All petrological results indicate that the CGD and CCG at the centre of the pluton could not be attributed to the contamination or crystallization differentiation due to in-situ cooling. Instead, from the weak variation trends in major and minor components, different characteristics in isotopes, plagioclase mineralogy and textures of the rocks, the

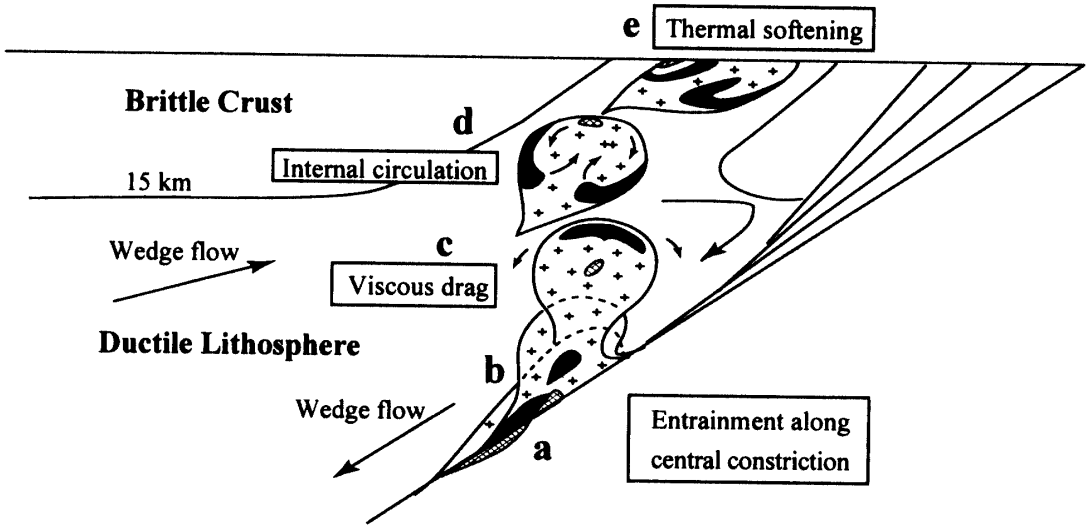

Fig. 8. Sketch showing a possible ascent path and evolution of the internal geometry of the Yakushima pluton rising through a ductile lithosphere from the top of the subducting slab. Entrainment of the initial basal layer (a and b) began after the overlying K-rich granite melts of later YMG reached sufficient volume to escape the viscous drag induced by the subducting slab (b and c). Viscous traction along the contact (c) induced internal toroidal circulation (d) and a doughnut-like compositional zoning during the buoyant rise of the detached diapir (e). The diapir rose obliquely toward the trench axis leaving a diapiric tail parallel to the subducting slab (d and e), because of the wedge flow induced in the overlying lithospheric wedge by shear along the top of the subducting slab. The brittle upper crust was weakened by the heat from the diapir (e).

magmas of the Yakushima pluton likely had different sources. We would tentatively attribute such a diversity of the source rocks and the compositional gradient that start from rather primitive YMG and ending up with the contaminated CCG now encased by the surrounding YMG, to the segregation of the granite melt from the subducted slab and sediments trapped by and sinking with it.

Our preferable model in which the Yakushima pluton rose diapirically and obliquely toward the inner wall of the Ryukyu Trench in the southeast (ANMA and SOKOUTIS, 1997) from the top of the subducting slab is illustrated in the Fig. 8. When the first bulge of the primitive and enriched YMG formed in the source layer due to partial melting of the slab (plus subducted sediments), the neighbouring depleted MFG, CGD and CCG (due mainly to the melting of sediments) were entrained into the YMG along its central constrictive flow (Fig. 8a, b). The different magmas, then, rose together and developed a doughnut-like compositional zoning in the pluton (Fig. 8e) due to internal circulation induced by viscous retardation (Fig. 8c, d). Since entrainment takes place when the viscosity contrast is low (JACKSON and TALBOT, 1989), this process must have occurred at depths where surrounding protoliths of the YMG were sufficiently hot to have viscosities similar to the YMG magma.

The compositional variation in the Yakushima pluton could be rationally explained by applying diapir model. High An contents in the CGD, CCG and MFG could also be attributed to the inhomogeneous heat distribution in a circulating fluid sphere (HEAD and

HELLUMS, 1966) superimposed over the concentric cooling. Such doughnut-like compositional zoning could be expected in a magmatic pluton that rose through a ductile media as a diapir.

7. Conclusion

(1) The core (CCG and CGD) and periphery parts (MFG) of the Yakushima pluton are per-aluminous cordierite granitoids. These are separated by the intervening cordierite-free granite (YMG) which is rather primitive in Nd-Sm and Rb-Sr isotopes and enriched in the incompatible elements. Thus, the Yakushima pluton has a doughnut-like compositional zoning.

(2) The CCG that is the most affected by the crustal protolith or sediments, and now exposed in the northwest of the pluton, cannot be attributed to the wall-rocks at the emplacement level, but deeper processes must have been involved.

(3) This doughnut-like zoning is symmetrical about an axis inclined to the NW and closely connected with the pattern of the magmatic flow. Neither nested pluton or ballooning pluton scenario is likely. This compositional zoning is attributed to the entrainment of minor crustal components into the main body of the YMG due to internal circulation driven by viscous retardation during the diapiric ascent of the Yakushima pluton. This diapir rose obliquely toward the Ryukyu trench axis in the southeast.

Acknowledgments

We express our thanks to Prof. SHIRAISHI and Dr. MOTOYOSHI who kindly arranged the symposium and gave us the opportunity to contribute this volume. Dr. MOTOYOSHI is also thanked for reviewing the paper. RA would like to express his gratitude to Prof. Christopher TALBOT for discussion and critical reading of early versions of this work. RA and YK would like to thank Prof. KIZAKI of the University of the Ryukyus for his discussion and guidance. Prof. KAGAMI is thanked for providing us equipment for isotope analyses. RA's thanks also go to Hans HARRYSON for assistance with electron probe microanalysis, and Christina WERNSTRÖM for preparation of figures.

References

ANMA, R. (1997): Oblique diapirism of the Yakushima granite in the Ryukyu arc, Japan. Granite: From Segregation of Melt to Emplacement Fabrics, ed. by J.L. BOUCHEZ *et al.* Dordrecht, Kluwer Academic, 295–318.

ANMA, R. and SOKOUTIS, D. (1997): Experiments on pluton shapes and tracks above subduction zones. Granite: From Segregation of Melt to Emplacement Fabrics, ed. by J.L. BOUCHEZ *et al.* Dordrecht, Kluwer Academic, 319–334.

ARAMAKI, S., HIRAYAMA, K. and NOZAWA, T. (1972): Chemical composition of Japanese granites, part 2: Variation trends and average composition of 1200 analyses. J. Geol. Soc. Jpn., **78**, 39–49.

BHATTACHARJI, S. (1967): Mechanics of flow differentiation in ultramafic and mafic sills. J. Geol., **75**, 101–112.

CHAPPELL, B.W. and WHITE, A.J.R. (1974): Two contrasting granite types. Pacific Geol., **8**, 173–174.

CRUDEN, A.R. (1990): Flow and fabric development during the diapiric rise of magma. J. Geol., **98**,

681-698.

CRUDEN, A.R., KOYI, H. and SCHMELING, H. (1995): Diapiric basal entrainment of mafic into felsic magma. Earth Planet. Sci. Lett., **131**, 321-340.

FINK, J.H. (1983): Structure and emplacement of a rhyolitic obsidian flow: Little Glass Mountain, Medicine Lake Highland, northern California. Geol. Soc. Am. Bull., **94**, 362-380.

FINK, J.H. and POLLARD, D.D. (1983): Structural evidence for dikes beneath silicic domes, Medicine Lake Highland Volcano, California. Geology, **11**, 458-461.

FRIDRICH, C.J. and MAHOOD, G.A. (1984): Reverse zoning in the resurgent intrusions of the Grizzly Peak cauldron, Swatch Range, Colorado. Geol. Soc. Am. Bull., **95**, 779-787.

HEAD, H.N. and HELLUMS, J.D. (1966): Heat transport and temperature distributions in large single drops at low Reynolds numbers: a new experimental technique. Am. Inst. Chem. Eng. J., **12**, 553-559.

ISHIHARA, S. (1977): The magnetite-series and ilmenite-series granitic rocks. Mining Geol., **27**, 293-305.

IWASAKI, T., HIRATA, N., KANAZAWA, T., MELLES, J., SUYEHIRO, K., URABE, T., MÖLLER, L., MAKRIS, J. and SHIMAMURA, H. (1990): Crustal and upper mantle structure in the Ryukyu Island Arc deduced from deep seismic sounding. Geophys. J. Int., **102**, 631-651.

JACKSON, M.P.A. and TALBOT, C.J.T. (1989): Anatomy of mushroom-shaped diapirs. J. Struct. Geol., **11**, 211-230.

KAGAMI, H., IWATA, M., SANO, S. and HONMA, H. (1987): Sr and Nd isotopic compositions and Rb, Sr, Sm and Nd concentration of standard samples. Tech. Rep. Inst. Study Earth Inter., Okayama Univ., Ser. B4, 1-16.

KAGAMI, H., YOKOSE, H. and HONMA, H. (1989): $^{87}Sr/^{86}Sr$ and $^{143}Nd/^{144}Nd$ ratios of GSJ rock reference samples; JB-1a, JA-1 and JG-1a. Geochem. J., **23**, 209-214.

KAWACHI, Y. and SATO, T. (1978): Orthoclase megacrysts in the Yakushima granite, southern Kyushu, Japan. Neues Jahrb. Mineral. Abh., **132**, 136-152.

KAWANO, Y. (1991): Geological and geochemical study of plutonic rocks in the Ryukyu arc, Japan. Niigata Univ. PhD thesis.

MARSH, B.D. (1988): Crystal capture, sorting and retention in convecting magma. Geol. Soc. Am. Bull., **100**, 1720-1737.

MITI (Ministry of International Trade and Industry) (1992): Report of potential investigation of rare metal mineral resources: the Yakushima area, 1991. Tokyo, Ministry of International Trade and Industry, 171 p. (in Japanese).

NAKATA, S. and TAKAHASHI, M. (1979): Regional variation in chemistry of the Miocene intermediate to felsic magmas in the Outer Zone and the Setouchi Province of Southwest Japan. J. Geol. Soc. Jpn., **85**, 571-582.

O'CORNER, J.T. (1965): A classification of quartz-rich igneous rocks based on feldspar ratios. U. S. Geol. Surv. Prof. Pap., **525B**, 79-84.

RAMSAY, J.G. (1989): Emplacement kinematics of a granite diapir: the Chindamora batholith, Zimbabwe. J. Struct. Geol., **11**, 191-209.

SATO, T. and NAGAHAMA, H. (1979): Geology of the Yakushima-seinanbu district. Geol. Surv. Japan, Quadrangle Series, Scale 1 : 50,000, Tanegashima (16), **9**, (in Japanese).

SATO, T., TERASHIMA, S. and ISHIHARA, S. (1982): Abundance of tin in the Yakushima granitic complex, southern Japan. J. Mineral. Petrol. Econ. Geol., **77**, 94-99.

SCHMELING, H., CRUDEN, A.R. and MARQUART, G. (1988): Finite deformation in and around a fluid sphere moving through a viscous medium: implications for diapiric ascent. Tectonophysics, **149**, 17-34.

SHIBATA, K. (1978): Contemporaneity of Tertiary granites in the Outer Zone of Southwest Japan. Bull Geol. Surv. Jpn., **29**, 551-554 (in Japanese).

SHIBATA, K. and NOZAWA, T. (1968): K-Ar ages of Yakujima Granite, Kyushu, Japan. Bull. Geol. Surv. Jpn., **19**, 237-241.

SHIMAMOTO, T. (1993): Rheology of rocks and plate tectonics. Comprehensive Rock Engineering, 1. Fundamentals, ed. by E.T. BROWN and J.A. HUDSON. Oxford, Pergamon Press, 93-109.

TAKAHASHI, M., ARAMAKI, S. and ISHIHARA, S. (1980): Magnetite-series/ilmenite-series vs. I-type/S-type granitoids. Min. Geol. Spec. Issue, **8**, 13–28.

TALBOT, C.J. and JACKSON, M.P.A. (1987): Internal Kinematics of salt diapirs. Am. Assoc. Pet. Geol. Bull., **71**, 1068–1093.

TERAKADO, Y., SHIMIZU, H. and MASUDA, A. (1988): Nd and Sr isotopic variations in acidic rocks formed under a peculiar tectonic environment in Miocene Southwest Japan. Contrib. Mineral. Petrol., **99**, 1–10.

WEINBERG, R.F. (1992): Internal circulation in a buoyant two-fluid Newtonian sphere: implications for composed magmatic diapirs. Earth Planet. Sci. Lett., **110**, 77–94.

WOODCOCK, N.H. (1977): Specification of fabric shapes using an eigenvalue method. Geol. Soc. Am. Bull., **88**, 1231–1236.

ZORPI, M.J., COULON, C., ORSINI, J.B. and COCIRTA, C. (1989): Magma mingling, zoning and emplacement in calk-alkaline granitoid plutons. Tectonophysics, **157**, 315–329.

(Received February 13, 1998; Revised manuscript accepted July 14, 1998)